

OXIDATION OF $TiC_{1-x}N_x$ CERAMIC POWDERS BY MULTIPLE THERMAL
ANALYSIS USING A NEWLY DEVELOPED POTENTIOMETRIC CO_2 SENSOR

Toshio Maruyama

Research Laboratory of Engineering Materials

Tokyo Institute of Technology

4259 Nagatsuta-cho, Midori-ku, Yokohama 227, Japan

ABSTRACT

The oxidation of $TiC_{1-x}N_x$ ($x=0-1$) ceramic powders has been examined by a multiple technique consisting of thermogravimetry (TG), differential thermal analysis (DTA) and evolved gas analysis (EGA) using a newly developed potentiometric CO_2 sensor. Sample except $x=1$ are oxidized above 420 K through the substitution of oxygen for carbon and nitrogen at lattice sites and the oxygen dissolution into the interstitial sites at the early stage, forming an amorphous oxide. The oxidation is enhanced by the heat of reaction, which raises the sample temperature, and results in the explosive oxidation at 700-760 K. This process gives an abrupt rise of the sample temperature to about 1150 K and almost completes the oxidation giving rutile. The sample of $x=1$ is oxidized with the formation of both anatase and rutile at the early stage, and the final product is rutile at the completion.

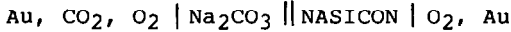
INTRODUCTION

Materials in $TiC-TiN$ system have been widely used as coatings for cutting tools because of their high hardness. Recently an attempt has been made to apply TiN to gate electrodes and interconnection in large-scale integrated circuits [1]. The performance of materials for these applications is strictly related to the oxidation resistance. The oxidation process of $TiC_{1-x}N_x$ involves the evolution of gaseous species such as CO_2 and N_2 . Furthermore, the dissolution of oxygen into the lattice may be important at the early stage of oxidation [2]. The mass gain in TG is caused by the dissolution of oxygen and the oxidation reaction to TiO_2 . Quantitative EGA which is conducted simultaneously with TG and DTA provides a valuable information to the analysis of such a complicated process.

In the present study, the oxidation process of $TiC_{1-x}N_x$ powders was investigated in oxygen by multiple thermal analysis consisting of TG, DTA and EGA with a newly developed potentiometric CO_2 sensor.

EXPERIMENTAL

Powders of $TiC_{1-x}N_x$ ($x=0, 0.3, 0.5, 0.7$ and 1 , grain sizes: $1-2 \mu m$) were provided by Japan New Metals Corp. The crystal structure of $TiC_{1-x}N_x$ was cubic and the spacing of (422) varied linearly from 8.836×10^{-2} ($x=0$) to 8.666×10^{-2} nm ($x=1$). The oxidation kinetics of the powders were examined by TG, DTA and EGA in oxygen stream of $2.67 \times 10^{-6} m^3 s^{-1}$. Samples of about 15 mg were weighed and set into the TG-DTA apparatus (SSC/560GH, Seiko Instruments and Electronics Ltd.). X-ray diffraction was conducted at various stages of oxidation. A potentiometric CO_2 sensor [3] was employed for EGA. The sensor is composed of Na_2CO_3 and NASICON ($Na_3Zr_2Si_2PO_{12}$) which are both sodium ion conductors, and described as the following electrochemical cell:



The electromotive force (emf: E) is expressed by the Nernst equation:

$$E = E_0 - (2.303 RT/2F) \log(a_{Na_2O} P_{CO_2} / 1.01 \times 10^5) \quad (1)$$

where E_0 is the constant, R the gas constant, T the absolute temperature, F the Faraday constant, a_{Na_2O} the activity of Na_2O in NASICON and P_{CO_2} the partial pressure of CO_2 in pascal. In the case of a fixed activity of Na_2O in NASICON, the partial pressure of CO_2 can be calculated from the measured emf. Figure 1 shows the typical emf characteristic of the sensor. As can be expected from the eqn. (1), the linear relationship is obtained between the emf and $\log(P_{CO_2})$.

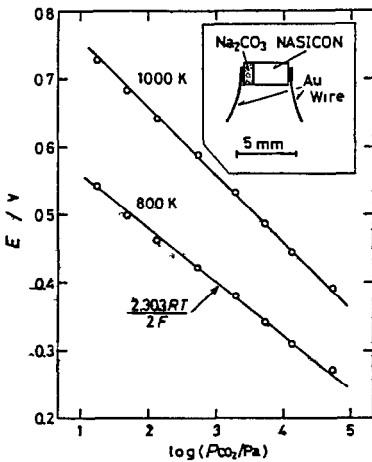


Fig. 1 Emf characteristic of the CO_2 sensor.

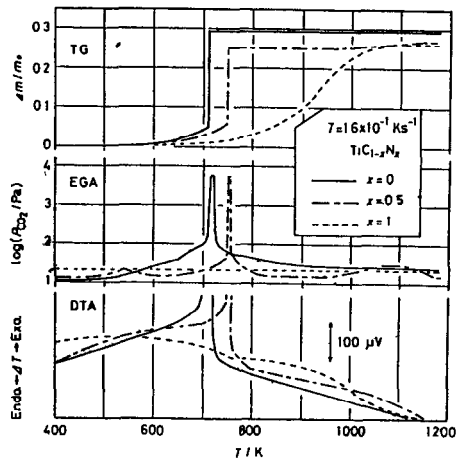


Fig. 2 TG, DTA and EGA curves ($\dot{T} = 1.6 \times 10^{-1} K s^{-1}$)

RESULTS AND DISCUSSION

Figure 2 shows typical curves of TG, DTA and EGA at a heating rate of $1.6 \times 10^{-1} \text{ Ks}^{-1}$. The CO_2 sensor was held at 900 K. For clearness of the figure, only three curves of $x=0, 0.5$ and 1 are presented. The TG curve of $x=0$ indicates that the mass gain starts at 520 K. The mass gain is gradually increased to 0.05 up to 710 K, and the explosive oxidation is observed at 710 K to attain the mass gain of 0.295. On the other hand, the EGA curve by the CO_2 sensor shows that the evolution of CO_2 begins at 420 K. The sensor is more sensitive than TG. The explosive oxidation increases the partial pressure of CO_2 to $5.5 \times 10^4 \text{ Pa}$. The explosive oxidation gives an abrupt rise of the sample temperature to 1150 K. As can be seen in the EGA curve of $x=0.5$, the evolution of CO_2 begins at 420 K, and a small peak is observed around 540 K. Then the amount of evolved CO_2 decreases with increasing temperature below 630 K, whereas TG shows a monotonous mass gain below 750 K at which the explosive oxidation occurs. The sample of $x=1$ provides a smooth TG curve. The CO_2 sensor exhibits no change in emf indicating the excellent selectivity. The DTA shows a broad exothermic peak from 760 K. Figure 3 presents TG, DTA and EGA curves at a heating rate of $5.0 \times 10^{-2} \text{ Ks}^{-1}$. The lowering of the heating rate eliminates the explosive behavior from the sample of $x=0.5$. Table 1 summarizes the temperatures and mass gains where the explosive oxidation occurs at various heating rates. The sample of higher carbon concentration explodes at lower temperatures and heating rates. However, mass gains remain less than about 0.1. DTA curves showed that the evolved heat decreased with an increase in x . X-ray diffraction revealed that no newly formed crystalline phase was detected before the explosive oxidation, and the change in the lattice constant of original phase was negligible in the samples of $x=0$ and 0.5 . The explosive oxidation converted them into rutile. The sample of $x=1$ yielded small amounts of anatase and rutile

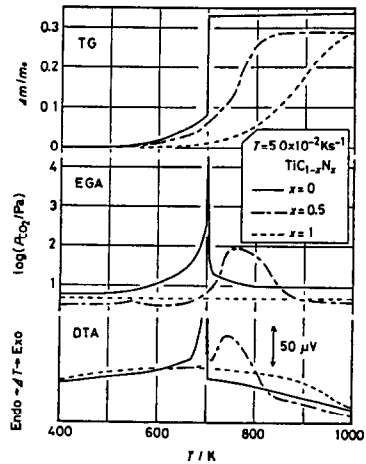


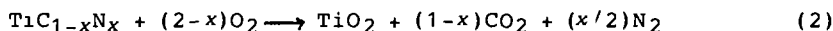
Fig. 3 TG, DTA and EGA curves ($\dot{T}=5.0 \times 10^{-2} \text{ Ks}^{-1}$).

Table 1 Temperatures and mass gains at the explosive oxidation. (T/K)/($\Delta m/m_0$)

\dot{T}/Ks^{-1}	x				
	0	0.3	0.5	0.7	1
1.6×10^{-1}	710/0.05	733/0.07	748/0.06	749/0.06	non
1.0×10^{-1}	713/0.05	738/0.08	758/0.11	741/0.08	non
7.5×10^{-2}	703/0.07	738/0.08	non	non	non
5.0×10^{-2}	700/0.08	non	non	non	non
2.5×10^{-2}	non	non	non	non	non

at mass gain of 0.08, and the anatase had been transformed into rutile until the oxidation was completed.

By assuming that the oxidation proceeds through the following reaction in which oxygen substitutes for carbon and nitrogen at the lattice sites:



the value of P_{CO_2} can be calculated from the observed TG curve and the flow rate of oxygen. The calculated and observed values are compared in Fig. 4 for the early stage of oxidation in the samples of $x=0$ and 0.5 at the heating rate of $1.6 \times 10^{-1} Ks^{-1}$. For $x=0$, the calculated value agrees roughly with the observed one, indicating that the oxidation proceeds mainly through the reaction (2). On the other hand, for $x=0.5$, a significant difference is recognized between the calculated and observed values, suggesting that the dissolution of oxygen into the interstitial sites is involved. In this stage, the sample is self-heated because the evolved heat due to oxidation overcomes the effluent heat from the sample holder, and then is explosively oxidized at 700-760 K.

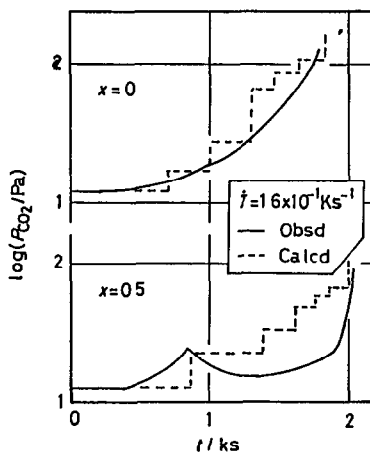


Fig. 4 Comparison of calculated and observed values of P_{CO_2} .

REFERENCES

- 1 M. Wittmer, J. Noser and H. Melchior, *J. Appl. Phys.*, 52 (1981) 6659.
- 2 V.A. Lavrenko, L.A. Glebov, A.p. Pomitkin, V.G. Chuprina and T.G. Protsenko, *Oxid. Met.*, 9 (1975) 171.
- 3 Y. Saito, T. Maruyama and S. Sasaki, Report of the research Laboratory of Engineering Materials, Tokyo Institute of Technology, 9 (1984) 17.